Changes in mean evapotranspiration dominate groundwater recharge in semi-arid regions

Tuvia Turkeltaub[1] and Golan Bel[2]

[1]Zuckerberg Institute for Water Research, Blaustein Institutes for Desert Research, Ben-Gurion University of the Negev, Sede Boqer Campus 8499000, Israel
[2]Department of Environmental Physics, Blaustein Institutes for Desert Research, Ben-Gurion University of the Negev, Sede Boqer Campus 8499000, Israel

Correspondence: Tuvia Turkeltaub (tuviat@bgu.ac.il)

Abstract. Groundwater is one of the most essential natural resources and is affected by climate variability. However, our understanding of the effects of climate on groundwater recharge (GR), particularly in dry regions, is limited. Future climate projections suggest changes in many statistical characteristics of the potential evapotranspiration (ETref) and the rainfall that dictates the GR. To better understand the relationship between climate statistics and GR, we separately considered changes to

5 the mean, STD, and extreme statistics of the ETref and the rainfall. We simulated the GR under different climate conditions in multiple semi-arid locations worldwide. We find that changes in the average ETref have the most significant impact on GR. Interestingly, we find that changes in the extreme ETref statistics have much weaker effects on the GR than changes in extreme rain statistics. Contradictory results of previous GR studies may be explained by the differences in the projected climate statistics.

1 Introduction

10 Groundwater sustainability depends on balancing groundwater recharge (GR) and groundwater abstraction (Hartmann et al., 2017; Wada et al., 2010). GR is the amount of water infiltrating the soil deep enough such that it is not lost to evaporation, transpiration, or runoff. Many areas across the globe show a growing dependence on groundwater resources, which will only increase in the future (Bierkens and Wada, 2019; Taylor et al., 2013a, b). Climate variability affects both the precipitation and

15 the evapotranspiration statistics. Therefore, understanding the potential effects of these factors on GR is of great importance. In order to improve groundwater resource management and reduce negative human effects (Taylor et al., 2013a), the direct influences of climate variability on GR must be quantified.

In recent years, much effort has been devoted to the analysis of the sensitivity of groundwater systems to climate change (Meixner et al., 2016; Pulido-Velazquez et al., 2015; Touhami et al., 2015; Fu et al., 2019; Döll and Fiedler, 2008; Tillman

20 et al., 2016; Reinecke et al., 2021; Huang et al., 2023; Berghuijs, 2024; Berghuijs et al., 2024). However, no conclusive generic outcomes can be drawn regarding the relationship between changes in climate conditions and the resulting changes in GR rates (Al Atawneh et al., 2021; Green et al., 2011). The main source of uncertainties in future GR is the uncertainties in climate predictions. It is unclear whether the climate variability is amplified or smoothed in the GR response (Taylor et al., 2013a; Field

et al., 2012; Reinecke et al., 2021; Moeck et al., 2016). Moreover, even the trend of the GR response is uncertain (Smerdon, 2017).

Climate variability may also change the seasonal distribution of the rain (Allan and Soden, 2008; Field et al., 2012). Increasing temperatures are expected to increase evapotranspiration (ET) (Condon et al., 2020) while the increased CO_2 concentrations are expected to lower the ET (Cao et al., 2010), and the overall effect is uncertain (Barnett et al., 2008). The future GR uncertainties are even more dominant in arid and semi-arid regions where the variability of the ET affects the threshold values for GR (Cuthbert et al., 2019b). Different studies have reached contradictory conclusions regarding the effects of climate change on GR in arid and semi-arid regions (Crosbie et al., 2013). Some studies found that the changes in GR are greater than the changes in climate conditions (Ng et al., 2010; McKenna and Sala, 2018), while others found weak sensitivity of semi-arid regions to climate variability (Döll and Fiedler, 2008; Cuthbert et al., 2019a). Under future climate conditions, the precipitation and potential ET (ETref) statistics and, particularly, the frequency of extreme events (Myhre et al., 2019) may change. The effects of these extreme events may lead to an increase (Taylor et al., 2013b, a; Cuthbert et al., 2019b; Shamsudduha and Taylor, 2020; Goni et al., 2021) or a decrease (Cuthbert et al., 2019b) in GR.

Previous studies investigated the GR response to predicted future climate conditions using global climate model (GCM) (Crosbie et al., 2013; Tillman et al., 2016) or regional GCM (Pulido-Velazquez et al., 2015) predictions. Pulido-Velazquez et al. (2015) also considered modifications of the mean and standard deviation (STD) of the rain in the regional GCM predictions. However, these studies could not provide a conclusive understanding of the effects; in particular, changes in the ETref statistics were not directly considered.

The main objective of this study is to explore the changes in diffuse (rather than focused, agricultural, or mountain, see Meixner et al. (2016)) GR in semi-arid and arid regions due to changes in rain and ETref statistics. In this study, GR is defined as the accumulated water flux at a 5 m depth, assuming that this flux reaches the water table. To enhance our understanding of the GR response to climate variability, we separately consider the changes in the mean, STD, and extreme events of ETref and rain statistics (relative to the measured statistics) in multiple locations across the globe. While we do not consider specific future climate projections we identify and quantify the effects of changes in climate variables statistics on GR in semi-arid regions.

2 Methods

We use a numerical model to simulate the GR under atmospheric boundary conditions. In what follows, we provide the details of the model, the independent data used for verification of the model, and the changes applied to the climate variables statistics.

2.1 Groundwater recharge data and modeling

To explore the impact of climate statistics on GR, we identified 200 semi-arid locations (supporting information (SI)) in which GR was estimated using ground-based methods such as chloride mass balance, water isotopes, etc. (Taylor et al., 2013b; Scanlon et al., 2006; Moeck et al., 2020). These locations span both hemispheres and different continents (see Fig. 1a). Furthermore,

they cover a wide range of soil types (Fig. 1b) and climate conditions, including various seasonal rain distributions relative to temperature and other factors affecting evapotranspiration. The locations are characterized by bare soil or sparse vegetation, where transpiration is negligible relative to the evaporation.

Diffuse GR fluxes were simulated using unsaturated flow modeling for these locations by numerically solving the 1D vertical Richards equation:

$$\frac{\partial \theta}{\partial t} = \frac{\partial}{\partial z}\left[K(\psi)\left(\frac{\partial \psi}{\partial z} + 1\right)\right], \tag{1}$$

where ψ is the matric potential head $[L]$, θ is the volumetric water content (dimensionless), t is time $[T]$, z is the vertical coordinate $[L]$, and $K(\psi)$ $[L\,T^{-1}]$ is the unsaturated hydraulic conductivity function. The Richards equation was numerically integrated using the Hydrus 1D (Šimůnek et al., 2009). Knowledge regarding the soil hydraulic functions is essential in order to solve the Richards equation. The soil retention curves and the unsaturated hydraulic curves are commonly described according to the van Genuchten-Mualem (VGM) model (Mualem, 1976; Van Genuchten, 1980):

$$S_e = \frac{\theta - \theta_r}{\theta_s - \theta_r} = \left[1 + (\alpha|\psi|)^n\right]^{-m}, \tag{2}$$

where S_e is the degree of saturation ($0 < S_e < 1$), θ_s and θ_r are the saturated and residual volumetric soil water contents, respectively, and α $[L^{-1}]$, n, and $m = (1 - 1/n)$ are shape parameters. Hydraulic conductivity is assumed to behave according to:

$$K(S_e) = K_s S_e^l \left[1 - \left[1 - S_e^{1/m}\right]^m\right]^2 \tag{3}$$

where K_s $[L\,T^{-1}]$ is the saturated hydraulic conductivity, and l is the pore connectivity parameter prescribed as 0.5.

The VGM parameters were determined using the pedo-transfer function ROSETTA (Zhang and Schaap, 2017), which uses a neural network to estimate the soil hydraulic parameters from soil attributes, such as soil texture and bulk density. Sand, silt, and clay contents and the bulk density were extracted at the considered locations from global soil maps reported by Hengl et al. (2014). Note that the data is divided into seven layers, but for the current study, only information from the top three layers was used (0–5, 5–15, and 15–30 cm; the VGM parameters are provided in SI). We assume that evaporation is mostly limited to the topsoil; therefore, we only considered the heterogeneity of these levels. Furthermore, the water table depths at the investigated locations, which were extracted from the global map presented by Fan et al. (2013), indicated that in most locations, groundwater is below 0.8 m depth and no phreatic evaporation is expected (SI; Chengcheng et al., 2020, Hellwig, 1973).

The water flow simulations were carried out using atmospheric boundary conditions with surface runoff. Daily precipitation and ETref (potential ET) values were specified at the upper boundary. The minimum allowed pressure head at the soil surface was constant (hCritA= 100000 cm). Lower boundary conditions were prescribed as free drainage, where the water flux across this boundary is considered the GR. The depth of the simulated soil column was 500 cm, and it was discretized into 101 grid cells. A finer node spacing was implemented at the upper boundary, where the top node was 3 times thinner than the bottom node. Water content at field capacity was prescribed as the initial condition at the start of each simulation. Each simulation was run for 146,100 days, and the calculated daily GR fluxes between days 73,050 and 146,100 were used for the analyses to avoid the influence of the initial conditions. In all the locations considered, the differences between the estimated and the observed GR/Rain ratios were below 5%, illustrating the suitability of the model.

2.2 Climate data and generation of rain and ETref time series

The CRU TS 3.2 climate dataset (Harris et al., 2014), including daily values of precipitation and potential evapotranspiration (ETref), was used for the analyses presented in the current study. The datasets were temporally downscaled, following van Beek (2008), to daily values using ERA40 (1958–1978, Uppala et al. (2005) and ERA-Interim (1979–2015, Dee et al. (2011)). The daily ETref values were calculated according to the Penman-Monteith method using climate variables such as mean, maximum, and minimum temperatures, vapour pressure, cloud cover, and wind speed (Harris et al., 2014). Stochastic rain and ETref time series spanning 400 years (146100 days) were synthesized based on these 58-year-long CRU TS 3.2 records of daily precipitation and potential evapotranspiration (ETref). Rain time series were established based on the empirical histograms of the number of rainy days and the daily rain amount distributions (SI; Turkeltaub and Bel, 2023). The ETref time series were established by random sampling of ETref empirical distributions for each calendar month separately (Turkeltaub and Bel, 2023). Furthermore, it was shown by the authors (Turkeltaub and Bel, 2023) that the best synthesis method involves a correction of the synthesized climate to match the observed monthly statistics. Thus, the rain and ET time series were corrected accordingly (see the examples in the SI Figs. S1 and S2 for the effects of the correction on the monthly rain and ETref statistics).

2.3 Modification of the mean (μ) and the standard deviation (STD, σ)

To examine the effects of changes in the statistics of the rain and the ETref time series on groundwater recharge (GR), the yearly mean, μ, and STD, σ, of these series were modified. Note that when we modify the average of a time series, the STD is conserved and vice versa. The modification of μ is simply conducted by adding to each value (in the rain series, only to non-zero values) in the original time series the difference between the original and modified yearly average divided by the number of relevant days in that year. Note that this correction could possibly have resulted in negative daily rain and ETref amounts when considering a reduction of the yearly averages. Therefore, for the ETref, only days with amounts above the correction were modified in order to ensure non-negative values of ETref for all days. For the rain series, we further wanted to conserve the statistics of the number of rainy days. Therefore, the maximal allowed reduction of rain sets the value to 1 mm/day (Turkeltaub and Bel, 2023). The modification of the STD is done in two stages. Firstly, each value in the original time
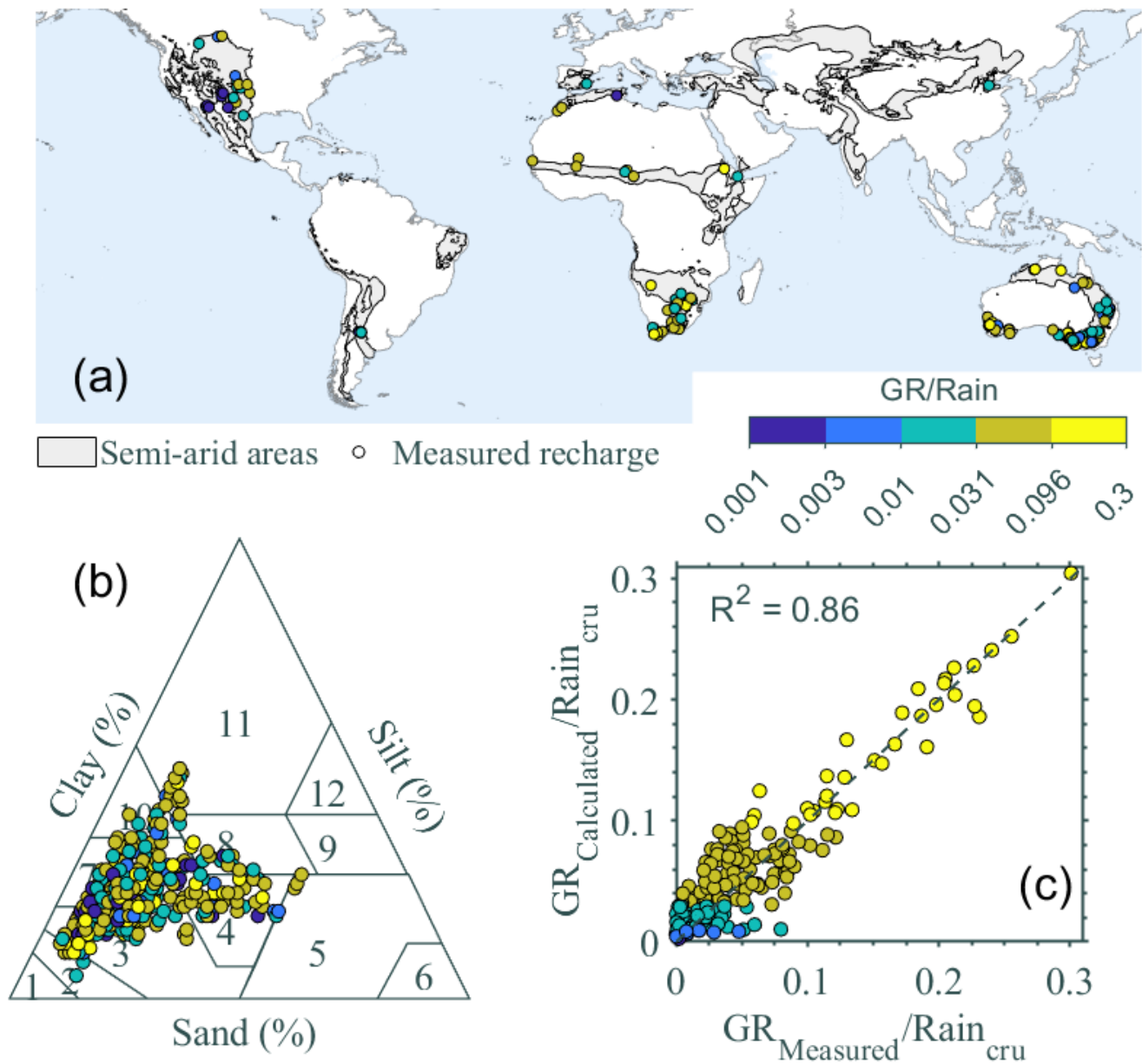
Figure 1. (a) The geographic distribution of the locations considered. (b) The soil composition, in terms of sand, silt, and clay, for all the locations considered in this study. The data are based on Hengl et al. (2014) and represent the reported soil characteristics for 0–5, 5–15, and 15–30 cm depths. (c) The simulated and reported ratio between the precipitation and the groundwater recharge for all the locations.

series is multiplied by the ratio between the original STD, σ_{org}, of the total yearly rain or the ETref and the modified STD, σ_{mf}. Subsequently, the differences between the averages of the original and the modified time series are corrected according to the procedure described above to preserve the original mean. Mathematically, the correction method for the annual μ of a time series is described as:

$$
\text{MTS}_\mu(t) = \begin{cases} \text{OTS}(t) \geq \text{Threshold} & \text{OTS}(t) + \frac{\Delta}{\text{Na(t)}} \\ \\ \text{OTS}(t) < \text{Threshold} & \text{OTS}(t) \end{cases} \tag{4}
$$

where MTS_μ and OTS are the modified mean and the original time series, respectively. Δ is the difference between the modified and the original annual rain or ETref averages ($\Delta \equiv \langle\text{MTS}_\mu\rangle_a - \langle\text{OTS}\rangle_a$, and $\langle.\rangle_a$ is the annual average of the variable represented in the time series). Na(t) is the number of days in the year of time t, with rain or ETref values larger than the threshold. The threshold is defined as $-\Delta/\text{Na(t)}$ for the ETref and as $-(\Delta/\text{Na(t)}+1)$ for the rain. Na(t) is found recursively.

To modify the σ of a time series, the following transformation is applied:

$$
\text{MTS}_\sigma(t) = \begin{cases} \text{OTS}(t) \times \frac{\sigma_m}{\sigma_o} \geq \text{Threshold} & \text{OTS}(t) \times \frac{\sigma_m}{\sigma_o} + \frac{\Delta_\sigma}{\text{Na(t)}} \\ \\ \text{OTS}(t) \times \frac{\sigma_m}{\sigma_o} < \text{Threshold} & \text{OTS}(t) \times \frac{\sigma_m}{\sigma_o} \end{cases} \tag{5}
$$

where σ_m and σ_o are the modified and original yearly standard deviation of the time series, respectively. $\Delta_\sigma \equiv \langle\text{OTS}\rangle_a \left(\frac{\sigma_m}{\sigma_o} - 1\right)$. The threshold is defined similarly to the definition above for the mean modification. Fig. 2 depicts an example of the modification of the average, μ, and STD, σ, of the yearly rain for a specific location ([-36.4469, 145.711]; (Crosbie et al., 2010)).

2.4 Modification of extreme events statistics

In order to increase the frequency of extreme events, the time series were modified such that the mean was conserved, and events above a specified quantile (0.98, 0.95, or 0.9) were doubled (Myhre et al., 2019; Fischer and Knutti, 2016). The doubling was done by randomly selecting events with values below the specified quantile and replacing their original value with a value from those above the quantile. We established two separate scenarios. The first doubles the frequency of the extreme events without preserving the seasonal cycle. Namely, an extreme event may be introduced into any day in the original series regardless of the season. In the second scenario, we preserve the seasonal cycle and double the extreme events for each calendar month separately. In the latter case, the added extreme events correspond to observed events in the same calendar month. For both scenarios, in order to preserve the annual mean, we used a procedure similar to the one outlined above for the annual mean modification (see eq. (4)).
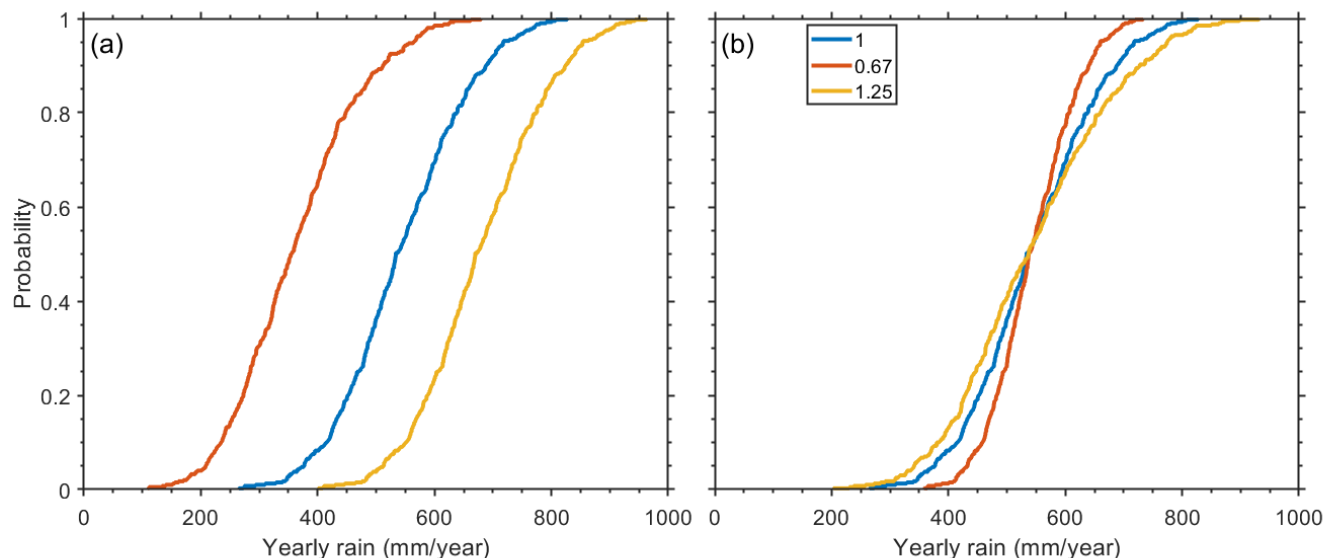
Figure 2. An example for the modification of the (a) mean, μ, and (b) the STD, σ, of a rain time series for a specific location where a groundwater recharge flux was reported ([-36.4469, 145.711]; (Crosbie et al., 2010)). The different colors correspond to the indicated modification factors.

For the rain time series, this was done without modifying the statistics of the number of rainy days; namely, only rainy days in the original time series could be randomly selected to receive one of the doubled extreme values. For the ETref time series, there was no additional constraint.

3 Results

3.1 Effects of changes in the mean

The first change we considered is a simple change in the mean (μ) of climatic variables (rain and ETref). Changes to the average ETref affect the GR/Rain ratio in all the locations (see Fig. 3). A larger mean ETref ($\mu_m/\mu_0 > 1$) reduces the GR/Rain ratio, while a smaller mean ETref ($\mu_m/\mu_0 < 1$) increases the ratio. The result is expected because the larger the actual ET (i.e., the estimated amount of water evaporated, determined by the numerical model; ETref $\geq$ actual ET), the smaller the ratio (in this case, the rain amount does not change). However, the change in the ratio is not the same for all locations, and obviously, it depends on the amount of water available for the actual ET and the amount of rain. It also suggests a nonlinear relation between the GR and rain rates. Histograms of the distribution of the change in the ratio, $\left(\frac{\text{GR}}{\text{Rain}}\right)_o - \left(\frac{\text{GR}}{\text{Rain}}\right)_m$ (the subscripts 0 and m correspond to the original and the modified ETref statistics, respectively), in the different locations, are depicted in Figure 4a-d. Some changes in the GR/R ratio are expressed by an increase or decrease of up to 20% in the fraction of rainfall

that becomes GR (Figure 4a-d). Note that the largest change in GR/R ratio occurs for a reduction of 0.67 of the mean annual ETref (Figure 4a).

Similarly, we considered changes in the mean rain (Fig. S3). The annual distribution of the rain is not modified, and only the amounts are increased or reduced by the desired multiplicative factor (see the Methods section for details; see also Fig.

165   2). In Fig. S3, the ratios, GR/Rain, under different changes to the mean rain, are shown. In general, reducing the rain results in a higher fraction of locations with a smaller GR/Rain ratio, while increasing the mean rain results in a higher fraction of locations with larger ratios. The histograms of the fraction of locations with different changes in the ratio (Figure 4e-h) reveal a more interesting response. Lowering the mean rain results in a mixed response. The GR/Rain ratio decreases in some locations, while it increases in others. In most locations with summer rain (92%, 73 of the considered locations), decreasing the mean

170   annual rain results in an increase in the ratio (Figure 4e,f). The GR in these locations is mostly a result of large rain events, and the decrease in the mean rain hardly affects the fraction of GR during these events.

3.2   Effects of changes in the STD

The second change in the statistics of the climate variables that we considered is a change to the STD of the variables while keeping the mean unchanged (see Fig. 2). This is equivalent to uniformly broadening the distribution of the ETref or the rain

175   (see the Methods section for details; Fig. 2). We find that increasing the STD of the ETref (Figs. S4) or the rain (Figs. S5) results in increasing the GR/Rain ratio in almost all the locations. This is also reflected by the change in the ratio, where most estimated GR/R ratios are larger than the original ratios, as indicated by the negative differences (Figure 4k,l,o,p).

Reducing the ETref (Figs. S4) or the rain (Figs. S5) STD reduces the GR/Rain ratio in most locations. This is illustrated by the positive values of the GR/R differences (Figure 4i,j,m,n). Overall, the reduction in the STD of the ETref or the rain has the

180   smallest effect on the GR/R ratio.

3.3   Effects of changes in the frequency of extreme events

Under some future climate predictions, the frequency of extreme events is expected to double (Myhre et al., 2019). Therefore, modifications of the extreme statistics as outlined in subsection 2.4 were considered. In Fig. 5, the histograms of the fraction of locations with specific GR/Rain ratios are depicted for the doubling of rain (panels (a) and (c)) and ETref (panels (b) and

185   (d)) extreme events above the 90%, 95%, and 98% quantiles. For reference, the panels also depict the histogram based on the measured climate conditions. It is apparent in panel (a) that doubling the extreme rain events results in more locations with higher GR/Rain ratios. Note that in this change, the total rain is not modified; therefore, the increase in the ratio implies an increase in the actual GR. The results are similar in panel (c) where the extreme events of each calendar month were doubled. In Fig. S6, the differences in GR/Rain are presented showing that for all the locations considered, increasing the frequency of

190   extreme events increases the GR despite the fact that the total rain is unchanged. Panel (b) shows that doubling the extreme ETref has a much smaller effect on the GR. Preserving the seasonality while doubling the extreme ETref events results in a somewhat stronger effect and more locations with higher GR as shown in panel (d) and Fig. S6. In panels (b) and (d) of Fig. S6, it is shown that in most locations, doubling the extreme ETref results in larger GR, while in a small fraction of the locations,
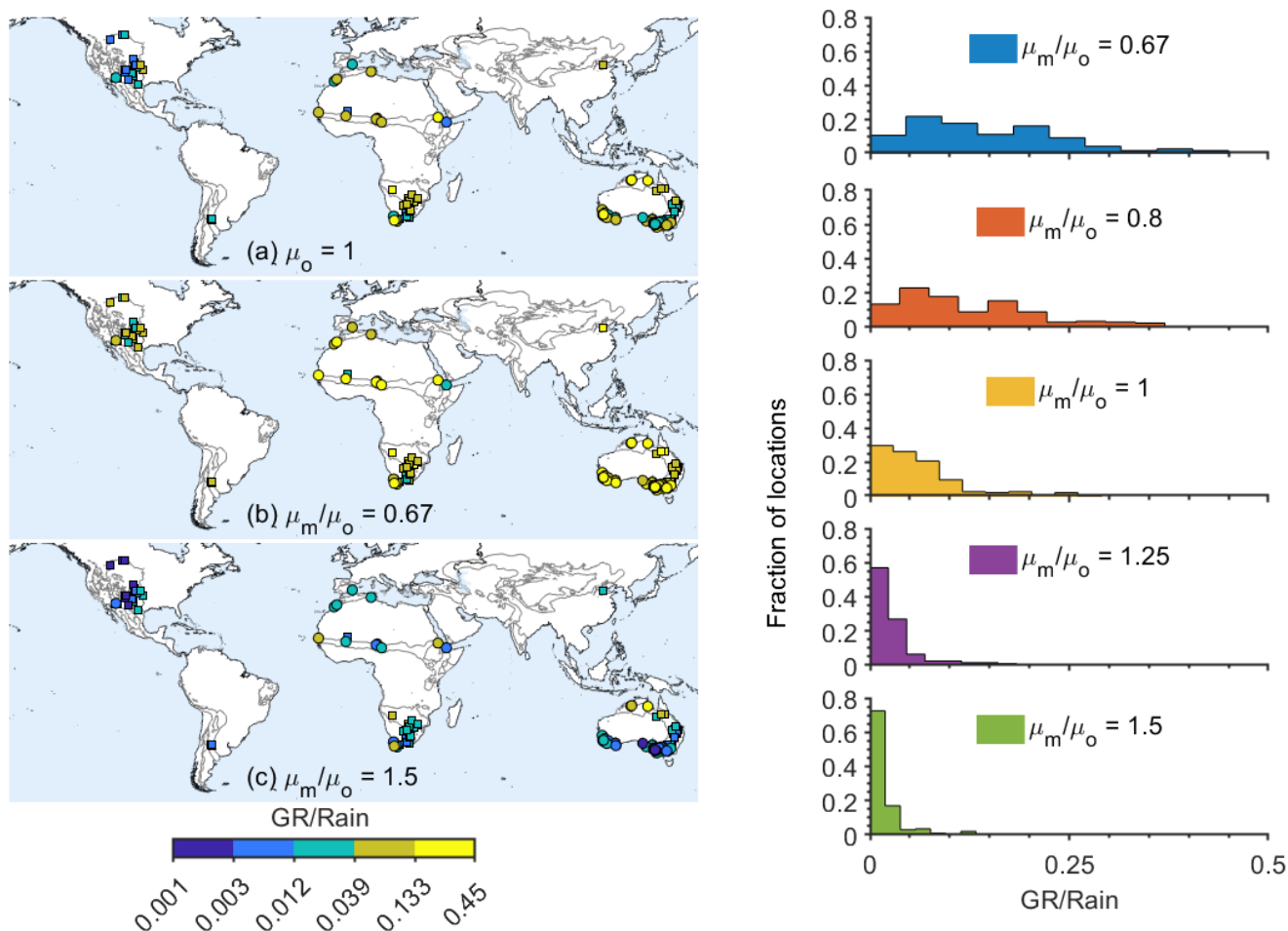
Figure 3. The effect of ETref yearly mean (μ) modification on the GR/Rain ratio. The left panels depict the modified ratio in different locations for the measured (top panel), reduced by a factor of 2/3 (middle panel) and increased by a factor of 1.5 (bottom panel), mean annual ETref, respectively. The right panels depict the histograms of the fraction of locations with different GR/Rain ratios under different mean ETref modifications. The ratios between the modified annual mean ETref (μ_m) and the original one (μ_0) are denoted in the figure.
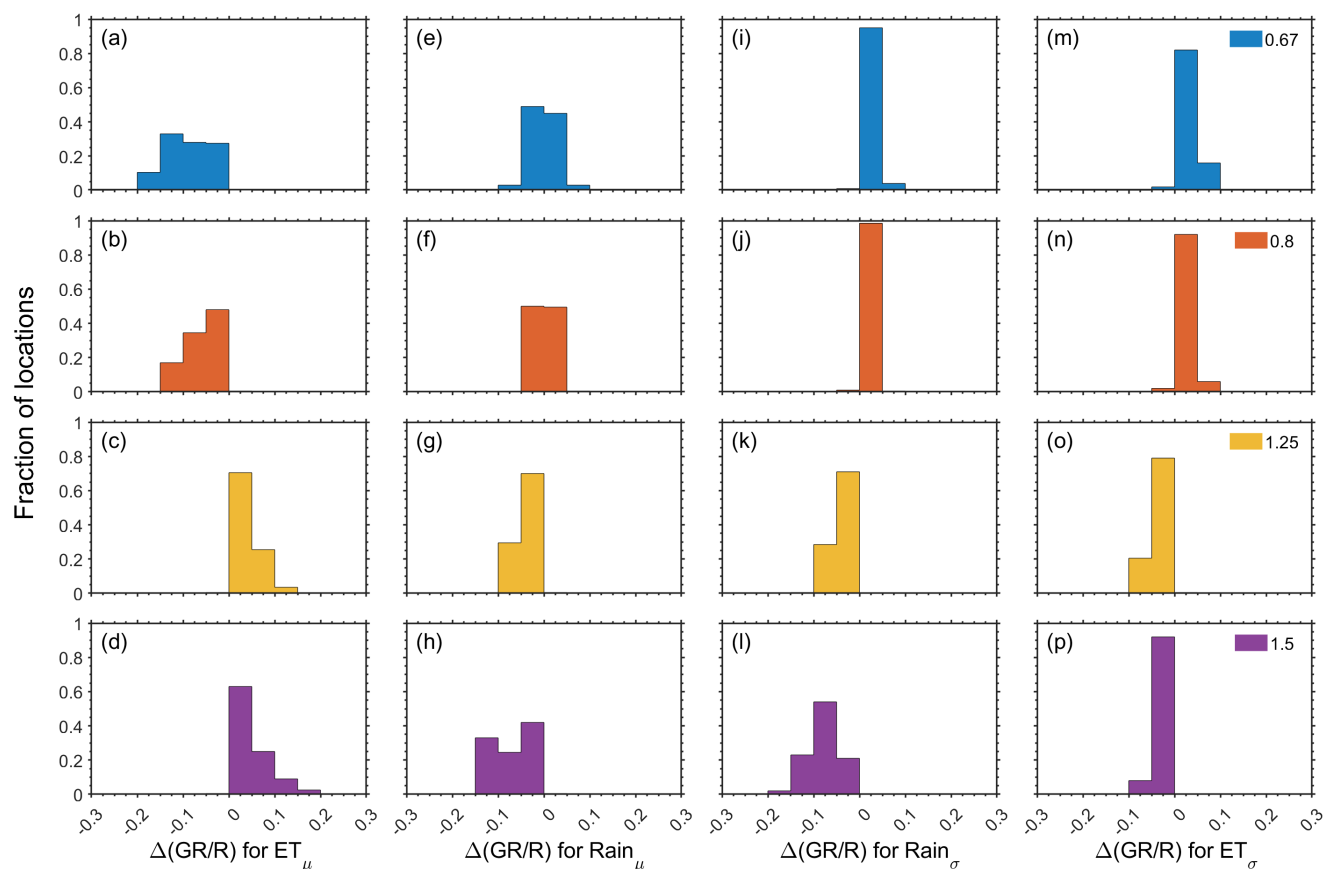
Figure 4. The panels depict the histograms of the change in the ratio GR/Rain (Δ(GR/R) = $\left(\frac{\text{GR}}{\text{Rain}}\right)_o - \left(\frac{\text{GR}}{\text{Rain}}\right)_m$; the subscripts o and m correspond to the original and the modified statistics, respectively) for changes in the (a-d) ETref yearly mean, (e-h) rain yearly mean, (i-l) rain yearly STD and (m-p) ETref yearly STD. The colors indicate the modification factors, which are the ratios between the modified annual mean (μ_m) or STD (σ_m) and the original one (μ_o) or STD (σ_o).

it reduces the GR. Note that these results differ from those of increasing the ETref STD for which all locations showed an
195   increase in the GR.

4   Discussion

Understanding the response of GR to varying climate conditions involves a broad range of possible changes to the statistics of
the climate variables and renders the task overly complicated. In our analyses above, we attempted to deal with this complexity
by separately considering different changes in climate statistics. Reducing the mean rain resulted in mixed outcomes. Some
200   locations illustrated a decrease in the GR/Rain ratio, while in others, it increased. The increase in the GR/R ratio mostly
occurred in locations with summer rain. Two main explanations are suggested for this counterintuitive change. The first reason
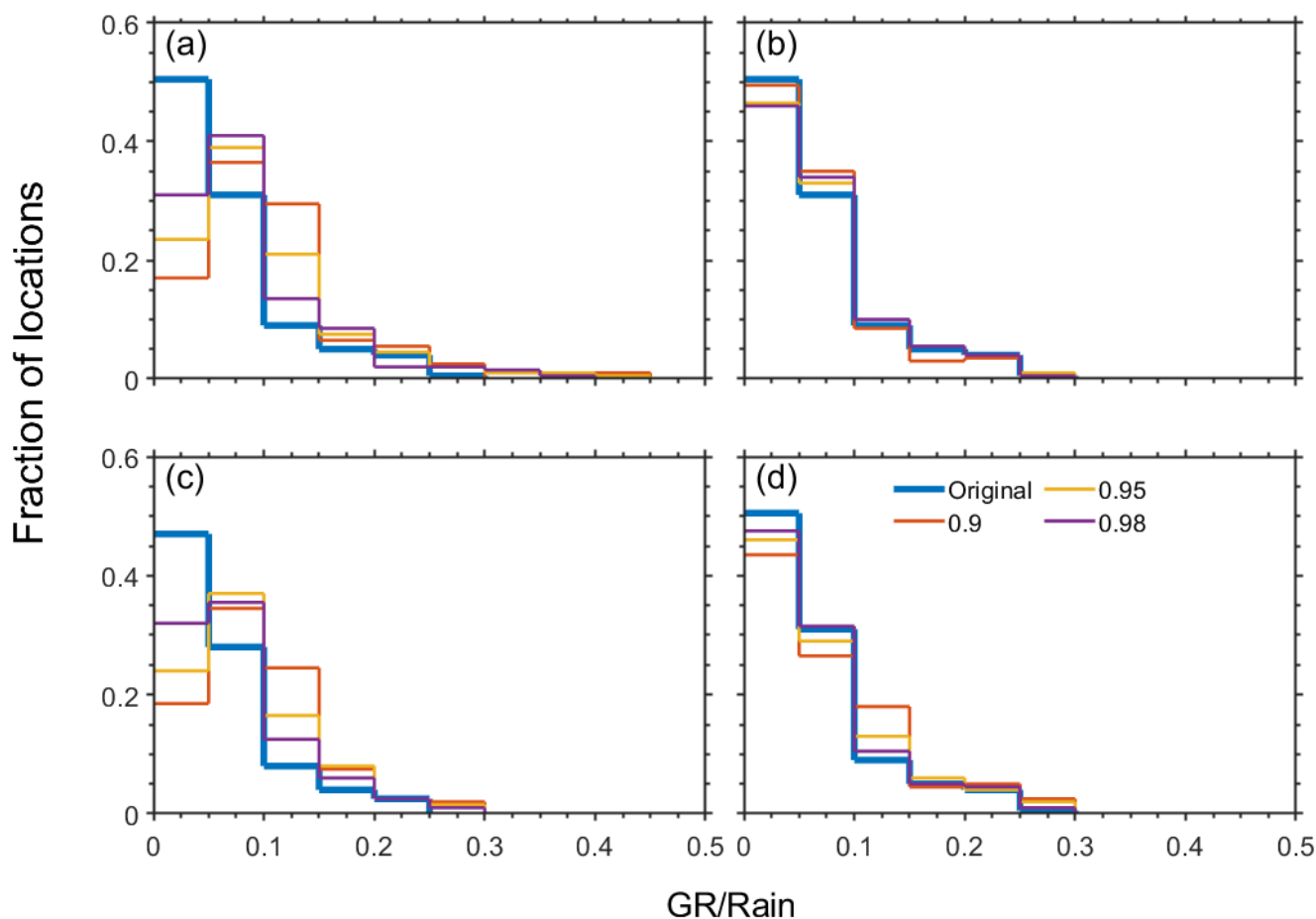
Figure 5. The fraction of locations with the specified GR/Rain ratios due to an increase in the occurrence of annual extreme (a) daily rain, or (b) daily ETref. The ratios due to an increase in the occurrence of extreme rain or ETref events for each calendar month separately are depicted in panels (c) and (d), respectively. See the Methods section for a detailed explanation of the changes to the extreme events statistics. The values of 0.98, 0.95, or 0.9 represent specified quantiles, where all events above the corresponding values were doubled to establish extreme climate scenarios. The blue line ('original') corresponds to scenarios with no changes to the extreme statistics.

is related to the rain characteristics in such regions of heavy rain events that promote deep drainage and GR. The decrease in the mean rain hardly affects the fraction of GR during these events. Therefore, the ratio is increased because the GR only decreases slightly, while the rain substantially decreases. An additional explanation is associated with the reduction of the

205   amount of water available for evaporation. The reduction of the amount of rain results in longer periods over which the actual ET is smaller than the potential ET, thereby increasing the fraction of rain going to the GR (in most days, the actual ET is either equal to the ETref when there is a continuum of water reaching the topsoil, or close to zero when there is not). Only 25% of the locations with winter rain showed the same behavior–most likely because the ET during the rainy season is relatively low in these locations, and the effect of the second process mentioned above is weaker. When the mean annual rain increases, all

210   locations show a larger GR/Rain ratio (see Fig.4e-h and Fig. S5).

We find that the GR/Rain ratio shows higher sensitivity to changes in the mean ETref than to changes in the mean annual rain. This is expected due to the following rationale. The rain is equal to the sum of the GR and actual ET under the assumption that in a steady state, the change in the soil water content is negligible and the assumption that the runoff is negligible (this was verified for the locations considered in this study). Mathematically, we express it as:

215
$$GR = R - ET,\tag{6}$$

and, therefore,

$$\frac{GR}{R} = 1 - \frac{ET}{R}.\tag{7}$$

The derivative of the ratio with respect to ET is:

$$\frac{d}{dET}\frac{GR}{R} = -1/R.\tag{8}$$

220   On the other hand, the derivative of the ratio with respect to R is:

$$\frac{d}{dR}\frac{GR}{R} = ET/R^2.\tag{9}$$

Assuming that the actual ET is proportional to the ETref implies a weaker sensitivity to changes in the average rain than to changes in the potential ET due to the factor of ET/R, which is smaller than 1, between the derivatives.

The response to changes in the rain STD is easily understood considering the fact that most of the GR is triggered by large

225   rain events. The increase in the GR/Rain ratio due to an increase in the ETref STD can be attributed to the fact that in some years, the ETref becomes small enough to allow significant GR, while during the years with higher ETref, the reduction in GR is much smaller because there is not always water available for actual ET, i.e., larger values of ETref do not affect the actual ET because it has already reached an upper limit. Ultimately, we found that changes in the statistics of extreme rainfall events have a much greater effect on GR than in extreme ETref events.

5   Conclusions

Understanding the combined effects of all the changes in climate variables on the GR is an ongoing effort and is expected to play a critical role in future studies. Our results suggest that in order to enhance our understanding and better explain the different GR responses reported in the literature, the results should be augmented by an analysis of the anticipated changes in ETref and rainfall statistics. As demonstrated above, considering only changes in the mean and the STD is not enough, and changes in the statistics of extreme events are essential. This is attributed to the nonlinear responses of the GR to changes in the climate variable statistics. The conclusions drawn in this analysis are valid for locations where diffuse recharge dominates GR. In areas where GR occurs predominantly through focused processes, future analyses should include additional factors at the sub-catchment scale, such as topographic attributes and spatiotemporal variability in precipitation. A separate study is required to investigate the effects of climate change on GR in humid regions or under agricultural fields, where the root uptake and the transpiration are significant.

Code availability.   The code used in this research will be made available upon a reasonable request.

Data availability.   The data used in this research will be made available upon a reasonable request.

Author contributions.   TT and GB designed the research, analyzed the data, and wrote the manuscript. TT performed the numerical simulations.

Competing interests.   The authors declare no competing interests.

References

Al Atawneh, D., Cartwright, N., and Bertone, E.: Climate change and its impact on the projected values of groundwater recharge: A review, Journal of Hydrology, 601, 126 602, https://doi.org/10.1016/j.jhydrol.2021.126602, 2021.

Allan, R. P. and Soden, B. J.: Atmospheric warming and the amplification of precipitation extremes, Science, 321, 1481–1484, https://doi.org/10.1126/science.1160787, 2008.

Barnett, T., Pierce, D., Hidalgo, H., Bonfils, C., Santer, B., Das, T., Bala, G.and Wood, A., Nozawa, T., Mirin, A., Cayan, D., and Dettinger, M.: Human-induced changes in the hydrology of western United States, Science, 319, 1080–1083, https://doi.org/10.1126/science.1152538, 2008.

Berghuijs, W. R.: An amplified groundwater recharge response to climate change, Nature Climate Change, pp. 1758–6798, 2024.

Berghuijs, W. R., Collenteur, R. A., Jasechko, S., Jaramillo, F., Luijendijk, E., Moeck, C., van der Velde, Y., and Allen, S. T.: Groundwater recharge is sensitive to changing long-term aridity, Nature Climate Change, pp. 1–7, 2024.

Bierkens, M. F. P. and Wada, Y.: Non-renewable groundwater use and groundwater depletion: a review, Environmental Research Letters, 14, 063 002, https://doi.org/10.1088/1748-9326/ab1a5f, 2019.

Cao, L., Bala, G., Caldeira, K., Nemani, R., and Ban-Weiss, G.: Importance of carbon dioxide physiological forcing to future climate change, Proceedings of the National Academy of Sciences, 107, 9513–9518, https://doi.org/10.1073/pnas.0913000107, 2010.

Chengcheng, G., Wenke, W., Zaiyong, Z., Hao, W., Jie, L., and Philip, B.: Comparison of field methods for estimating evaporation from bare soil using lysimeters in a semi-arid area, Journal of Hydrology, 590, 125 334, https://doi.org/10.1016/j.jhydrol.2020.125334, 2020.

Condon, L. E., Atchley, A. L., and Maxwell, R. M.: Evapotranspiration depletes groundwater under warming over the contiguous United States, Nature communications, 11, 1–8, https://doi.org/10.1038/s41467-020-14688-0, 2020.

Crosbie, R. S., Jolly, I. D., Leaney, F. W., and Petheram, C.: Can the dataset of field based recharge estimates in Australia be used to predict recharge in data-poor areas?, Hydrology and Earth System Sciences, 14, 2023–2038, https://doi.org/10.5194/hess-14-2023-2010, 2010.

Crosbie, R. S., Pickett, T., Mpelasoka, F. S., Hodgson, G., Charles, S. P., and Barron, O. V.: An assessment of the climate change impacts on groundwater recharge at a continental scale using a probabilistic approach with an ensemble of GCMs, Climatic Change, 117, 41–53, https://doi.org/10.1007/s10584-012-0558-6, 2013.

Cuthbert, M. O., Gleeson, T., Moosdorf, N., Befus, K. M., Schneider, A., Hartmann, J., and Lehner, B.: Global patterns and dynamics of climate–groundwater interactions, Nature Climate Change, 9, 137–141, https://doi.org/10.1038/s41558-018-0386-4, 2019a.

Cuthbert, M. O., Taylor, R. G., Favreau, G., Todd, M. C., Shamsudduha, M., Villholth, K. G., MacDonald, A. M., Scanlon, B. R., Valerie Kotchoni, D. O., Jean-Michel, V., Lawson, F. M. A., Adjomayi, P. A., Japhet, K., Seddon, D., Sorensen, J. P. R., Ebrahim, G. Y., Owor, M., Nyenje, P. M., Nazoumou, Y., Goni, I., Ousmane, B. I., Tenant, S., Ascott, M. J., Macdonald, D. M. J., Agyekum, W., Koussoubé, Y., Wanke, H., Kim, H., Wada, Y., Lo, M.-H., Oki, T., and Kukuric, N.: Observed controls on resilience of groundwater to climate variability in sub-Saharan Africa, Nature, 572, 230–234, https://doi.org/10.1038/s41586-019-1441-7, 2019b.

Dee, D. P., Uppala, S. M., Simmons, A. J., Berrisford, P., Poli, P., Kobayashi, S., Andrae, U., Balmaseda, M. A., Balsamo, G., Bauer, P., Bechtold, P., Beljaars, A. C. M., van de Berg, I., Biblot, J., Bormann, N., Delsol, C., Dragani, R., Fuentes, M., Greer, A. J., Haimberger, L., Healy, S. B., Hersbach, H., Holm, E. V., Isaksen, L., Kallberg, P., Kohler, M., Matricardi, M., McNally, A. P., Mong-Sanz, B. M., Morcette, J.-J., Park, B.-K., Peubey, C., de Rosnay, P., Tavolato, C., Thepaut, J. N., and Vitart, F.: The ERA-Interim reanalysis: Configuration and performance of the data assimilation system, Quarterly Journal of the Royal Meteorological Society, 137, 553–597, https://doi.org/10.1002/qj.828, 2011.

Döll, P. and Fiedler, K.: Global-scale modeling of groundwater recharge, Hydrology and Earth System Sciences, 12, 863–885, https://doi.org/10.5194/hess-12-863-2008, 2008.

285   Fan, Y., Li, H., and Miguez-Macho, G.: Global patterns of groundwater table depth, Science, 339, 940–943, https://doi.org/10.1126/science.1229881, 2013.

Field, C. B., Barros, V., Stocker, T. F., Dahe, Q., Dokken, D. J., Ebi, K. L., Mastrandrea, M. D., Mach, K. J., Plattner, G. K., Allen, S. K., Tignor, M., and Midgley, P. M.: Managing the risks of extreme events and disasters to advance climate change adaptation,Special Report of Working Groups I and II of the Intergovernmental Panel on Climate Change (IPCC), Cambridge University Press, https://www.ipcc.ch/
290   site/assets/uploads/2018/03/SREX_Full_Report-1.pdf[Accessed12August2023], 2012.

Fischer, E. M. and Knutti, R.: Observed heavy precipitation increase confirms theory and early models, Nature Climate Change, 6, 986–991, https://doi.org/10.1038/NCLIMATE3110, 2016.

Fu, G., Crosbie, R. S., Barron, O., Charles, S. P., Dawes, W., Shi, X., Niel, T. V., and Li, C.: Attributing variations of temporal and spatial groundwater recharge: A statistical analysis of climatic and non-climatic factors, Journal of Hydrology, 568, 816–834,
295   https://doi.org/10.1016/j.jhydrol.2018.11.022, 2019.

Goni, I. B., Taylor, R. G., Favreau, G., Shamsudduha, M., Nazoumou, Y., and Ngatcha, B. N.: Groundwater recharge from heavy rainfall in the southwestern Lake Chad Basin: evidence from isotopic observations, Hydrological Sciences Journal, 66, 1359–1371, https://doi.org/10.1080/02626667.2021.1937630, 2021.

Green, T. R., Taniguchi, M., Kooi, H., Gurdak, J. J., Allen, D. M., Hiscock, K. M., Treidel, H., and Aureli, A.: Beneath the surface of global
300   change: Impacts of climate change on groundwater, Journal of Hydrology, 405, 532–560, https://doi.org/10.1016/j.jhydrol.2011.05.002, 2011.

Harris, I., Jones, P., Osborn, T., and Lister, D.: Updated high-resolution grids of monthly climatic observations – the CRU TS3.10 Dataset, International journal of climatology, 34.3, 623–642, https://doi.org/10.1002/joc.3711, 2014.

Hartmann, A., Gleeson, T., Wada, Y., and Wagener, T.: Enhanced groundwater recharge rates and altered recharge sensitivity to climate
305   variability through subsurface heterogeneity, Proceedings of the National Academy of Sciences of the United States of America, 114, 2842–2847, https://doi.org/10.1073/pnas.1614941114, 2017.

Hellwig, D.: Evaporation of water from sand, 4: the influence of the depth of the water-table and the particle size distribution of the sand, Journal of Hydrology, 18, 317–327, https://doi.org/10.1016/0022-1694(73)90055-3, 1973.

Hengl, T., De Jesus, J. M., MacMillan, R. A., Batjes, N. H., Heuvelink, G. B., Ribeiro, E., Samuel-Rosa, A., Kempen, B., Leenaars,
310   J. G., Walsh, M. G., and Gonzalez, M. R.: SoilGrids1km - Global soil information based on automated mapping, PLoS ONE, 9, https://doi.org/10.1371/journal.pone.0105992, 2014.

Huang, Z., Yuan, X., Sun, S., Leng, G., and Tang, Q.: Groundwater Depletion Rate Over China During 1965–2016: The Long-Term Trend and Inter-annual Variation, Journal of Geophysical Research: Atmospheres, 128, e2022JD038 109, 2023.

McKenna, O. P. and Sala, O. E.: Groundwater recharge in desert playas: current rates and future effects of climate change, Environmental
315   Research Letters, 13, 014 025, https://doi.org/10.1088/1748-9326/aa9eb6, 2018.

Meixner, T., Manning, A. H., Stonestrom, D. A., Allen, D. M., Ajami, H., Blasch, K. W., E., A., Brookfield, and et al.: Implications of projected climate change for groundwater recharge in the western United States, Journal of Hydrology, 534, 124–138, https://doi.org/10.1016/j.jhydrol.2015.12.027, 2016.

Moeck, C., Brunner, P., and Hunkeler, D.: The influence of model structure on groundwater recharge rates in climate-change impact studies,
320   Hydrogeology Journal, 24, 1171, https://doi.org/10.1007/s10040-016-1367-1, 2016.

Moeck, C., Grech-Cumbo, N., Podgorski, J., Bretzle, A., Gurdak, J. J., Berg, M., and Schirmer, M.: A global-scale dataset of direct natural groundwater recharge rates: A review of variables, processes and relationships, Science of the Total Environment, 717, 137 042, https://doi.org/10.1016/j.scitotenv.2020.137042, 2020.

Mualem, Y.: A New Model for Predicting the Hydraulic Conductivity of Unsaturated Porous Media, Water Resources Research, 12, 513–522, https://doi.org/10.1029/WR012i003p00513, 1976.

Myhre, G., Alterskjær, K., Stjern, C. W., Hodnebrog, Ø., Marelle, L., Samset, B. H., Sillmann, J., Schaller, N., Fischer, E., Schulz, M., et al.: Frequency of extreme precipitation increases extensively with event rareness under global warming, Scientific reports, 9, 16 063, https://doi.org/10.1038/s41598-019-52277-4, 2019.

Ng, G.-H. C., McLaughlin, D., Entekhabi, D., and Scanlon, B. R.: Probabilistic analysis of the effects of climate change on groundwater recharge, Water Resources Research, 46, https://doi.org/10.1029/2009WR007904, 2010.

Pulido-Velazquez, D., García-Aróstegui, J. L., Molina, J. L., and Pulido-Velazquez, M.: Assessment of future groundwater recharge in semi-arid regions under climate change scenarios (Serral-Salinas aquifer, SE Spain). Could increased rainfall variability increase the recharge rate?, Hydrological Processes, 29, 828–844, https://doi.org/10.1002/hyp.10191, 2015.

Reinecke, R., Müller Schmied, H., Trautmann, T., Andersen, L. S., Burek, P., Flörke, M., Gosling, S. N., Grillakis, M., Hanasaki, N., Koutroulis, A., Pokhrel, Y., Thiery, W., Wada, Y., Yusuke, S., and Döll, P.: Uncertainty of simulated groundwater recharge at different global warming levels: a global-scale multi-model ensemble study, Hydrology and Earth System Sciences, 25, 787–810, https://doi.org/10.5194/hess-25-787-2021, 2021.

Scanlon, B. R., Keese, K. E., Flint, A. L., Flint, L. E., Gaye, C. B., Edmunds, W. M., and Simmers, I.: Global synthesis of groundwater recharge in semiarid and arid regions, Hydrological Processes, 20, 3335–3370, https://doi.org/10.1002/hyp.6335, 2006.

Shamsudduha, M. and Taylor, R. G.: Groundwater storage dynamics in the world's large aquifer systems from GRACE: uncertainty and role of extreme precipitation, Earth System Dynamics, 11, 755–774, https://doi.org/10.5194/esd-11-755-2020, 2020.

Šimůnek, J., Van Genuchten, M. T., and Šejna, M.: The HYDRUS software package for simulating the two-and three-dimensional movement of water, heat, and multiple solutes in variably-saturated porous media, Dep. Environmental Sciences, Univ. Calif., Riverside, CA., version 4.08. HYDRUS Software Series 3., 2009.

Smerdon, B. D.: A synopsis of climate change effects on groundwater recharge, Journal of Hydrology, 555, 125–128, https://doi.org/10.1016/j.jhydrol.2017.09.047, 2017.

Taylor, R. G., Scanlon, B., Döll, P., Rodell, M., Van Beek, R., Wada, Y., Longuevergne, L., Leblanc, M., Famiglietti, J. S., Edmunds, M., Leonard, K., Timothy, R. G., Jianyao, C., Makoto, T., Marc, F. P. B., Alan, M., Fan, Y., Reed, M. M., Yossi, Y., Gurdak, J. J., Allen, D. M., Shamsudduha, M., Hiscock, K., Yeh, P. J.-F., Holman, I., and Treidelothers, H.: Ground water and climate change, Nature climate change, 3, 322–329, https://doi.org/10.1038/nclimate1744, 2013a.

Taylor, R. G., Todd, M. C., Kongola, L., Maurice, L., Nahozya, E., Sanga, H., and MacDonald, A. M.: Evidence of the dependence of groundwater resources on extreme rainfall in East Africa, Nature Climate Change, 3, 374–378, https://doi.org/10.1038/nclimate1731, 2013b.

Tillman, F. D., Gangopadhyay, S., and Pruitt, T.: Changes in groundwater recharge under projected climate in the upper Colorado River basin, Geophysical Research Letters, 43, 6968–6974, 2016.

Touhami, I., Chirino, E., Andreu, J. M., Sánchez, J. R., Moutahir, H., and Bellot, J.: Assessment of climate change impacts on soil water balance and aquifer recharge in a semiarid region in south east Spain, Journal of Hydrology, 527, 619–629, https://doi.org/10.1016/j.jhydrol.2015.05.012, 2015.

Turkeltaub, T. and Bel, G.: The effects of rain and evapotranspiration statistics on groundwater recharge estimations for semi-arid environ-
360   ments, Hydrology and Earth System Sciences, 27, 289–302, https://doi.org/10.5194/hess-27-289-2023, 2023.

Uppala, S. M., Kållberg, P. W., Simmons, A. J., Andrae, U., Da Costa Bechtold, V., Fiorino, M., Gibson, J., Haseler, J., Her-nandez, A.,
       Kelly, G. A., Li, X., Onogi, K., Saarinen, S., Sokka, N., Allan, R. P., Anderson, E., Arpe, K., Balmaseda, M. A., Beljaars, A. C. M., Van
       De Berg, L., Bidlot, J., Bormann, N., Caires, S., Chevallier, F., Dethof, A., Dragosavac, M., Fisher, M., Fuentes, M., Hagemann, S., Hólm,
       E., Hoskins, B. J., Isaksen, L.and Janssen, P. A. E. M., Jenne, R., Mcnally, A. P., Mahfouf, J.-F., Morcrette, J.-J., Rayner, N. A., Saunders,
365   R. W., Simon, P., Sterl, A., Trenbreth, K. E., Untch, A., Vasiljevic, D., Viterbo, P., and Woollen, J.: The ERA-40 re-analysis, Quarterly
       Journal of the Royal Meteorological Society, 131, 2961–3012, https://doi.org/10.1256/qj.04.176, 2005.

van Beek, L. P. H.: Forcing PCR-GLOBWB with CRU data, Tech. Rep., https://vanbeek.geo.uu.nl/suppinfo/vanbeek2008.pdf, [Online;
       accessed 12-August-2023], 2008.

Van Genuchten, M. T.: A closed-form equation for predicting the hydraulic conductivity of unsaturated soils, Soil science society of America
370   journal, 44, 892–898, https://doi.org/10.2136/sssaj1980.03615995004400050002x, 1980.

Wada, Y., Van Beek, L. P., Van Kempen, C. M., Reckman, J. W., Vasak, S., and Bierkens, M. F.: Global depletion of groundwater resources,
       Geophysical Research Letters, 37, 1–5, https://doi.org/10.1029/2010GL044571, 2010.

Zhang, Y. and Schaap, M.: Weighted recalibration of the Rosetta pedotransfer model with improved estimates of hydraulic parameter distri-
       butions and summary statistics (Rosetta3), Journal of Hydrology, 547, 39–53, https://doi.org/10.1016/j.jhydrol.2017.01.004, 2017.